

Orbital order, stacking defects and spin- fluctuations in the p-electron molecular solid RbO_2

E. R. Ylvisaker, R. R. P. Singh, and W. E. Pickett

Department of Physics, University of California, Davis, California, 95616

(Dated: February 22, 2024)

We examine magnon and orbital behavior in localized O_2 anti-bonding molecular orbitals using an effective Kugel-Khomskii Hamiltonian derived from a two band Hubbard model with hopping parameters taken from ab initio density functional calculations. The considerable difference between intraband and interband hoppings leads to a strong coupling between the spin wave dispersion and the orbital ground state, providing a straightforward way of experimentally determining the orbital ground state from the measured magnon dispersion. The near degeneracy of different orbital ordered states leads to stacking defects which further modulate spin- fluctuation spectra. Proliferation of orbital domains disrupts long-range magnetic order, thus causing a significant reduction in the observed Neel temperature.

PACS numbers: 71.10.Fd, 75.10.Jm, 75.25.Dk, 75.50.Xx

Correlated systems have generated considerable interest in the literature in recent years. The discovery of high temperature superconductors and the subsequent development and application of correlated methods like LDA+U [1] and DMFT [2], has led to remarkable success in dealing with strongly correlated systems. At integer filling, strongly correlated systems are typically insulating and often show antiferromagnetic behavior arising from exchange or superexchange processes. Such systems include the undoped cuprates, where there is one hole per site that can hop in a square lattice of $\text{Cu d}_{x^2-y^2}$ orbitals, and heavy fermion materials like CeCuIn_5 where the Ce 4f orbitals weakly couple to the valence states. Multi-band correlated systems can also show orbital ordering; the earliest successful application of LDA+U found orbital ordering in the KCuF_3 system [3].

Since correlated behavior is typically the domain of materials with 3d and 4f orbitals, comparatively little attention has been given to the study of correlated behavior in p-orbital systems. However, local moment magnetism in 2p orbitals has been implicated in several systems, such as at polar oxide vacancies [4] and substitutionals [5]. The occurrence of 2p orbital moments at p-type $\text{LaAlO}_3/\text{SrTiO}_3$ interfaces [6] is still the only viable explanation of the insulating character that is observed in these interfaces, where the electron count would suggest metallic interface states. Alkali hyperoxides, to be discussed below, comprise another likely example. Recent calculations [7] suggest that doping of d^0 (no d electrons) magnetic systems can stabilize or even enhance 2p magnetic moments in systems such as ZnO nanowires [7].

Recently, there has been significant interest in studying correlations in solid molecular systems, such as SrN [8], which consists of Sr octahedra containing either isolated N atoms or N_2 dimers, with calculations predicting that the magnetic moment is strongly connected to the anionic N_2^{2-} dimers. Calculations on the Rb_4O_6 system [9] and Cs_4O_6 [10] suggest that these systems would be a half-

metallic ferromagnets particularly useful for spintronic applications, due to the reduced spin-orbit interaction in p-orbitals. However, these calculations were done with weakly correlated density functional theory; more recent calculations using LDA+U [11] suggest that the valence charge separates to give a mixture of magnetic hyperoxide O_2^- anions and nonmagnetic peroxide O_2^{2-} anions, and an insulating ground state. There seems to be some experimental disagreement as to whether Rb_4O_6 is conducting [12] or insulating [11]. In Rb_4O_6 the three different orientations of the O_2 dimers along the principle axes of the crystal give rise to frustration of the magnetic order.

Our interest here is in the alkali hyperoxides, taking RbO_2 as a specific example. Solov'yev [13] has provided a study of the sister compound KO_2 , considering the large spin-orbit coupling (SOC) limit. We present here an alternative viewpoint for RbO_2 , based on the supposition that SOC is not so large an effect, so orbital moments are quenched by the crystal field, making the conventional real p_x, p_y orbitals the natural basis for studying spin and orbital phenomena in RbO_2 . Experimental measurement of the Lande g-factor [14] yields values close to 2, indicating a mostly spin moment, rather than the $g = 4 = 3$ value expected for large spin-orbit coupling.

The MO_2 systems ($M = \text{Li, Na, Rb, Cs}$) exhibit complex phase diagrams and low temperature antiferromagnetism [15]. The phase diagrams at low temperature consist of several structural changes which are minor symmetry lowering distortions from the room temperature (averaged) tetragonal phase which is comparable to a distorted rock salt structure with O_2 ions playing the role of the anion, with the molecular axis pointing along the c direction, shown in Fig. 1b. The Jahn-Teller effect causes the O_2 molecules to tilt away from the tetragonal axis, an effect which is difficult to reproduce in a non-magnetic LDA calculation. Below 194 K, RbO_2 shows incommensurate superstructure and a mixture of pseudotetragonal,

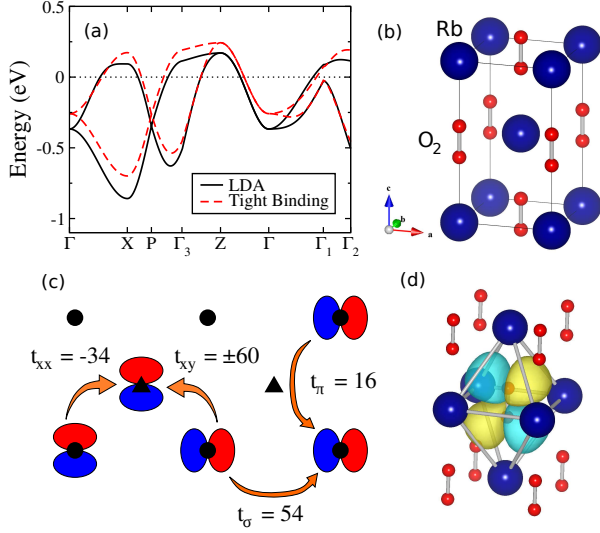


FIG. 1. (Color online) (a) Paramagnetic band plot of RbO_2 showing bands at the Fermi level from both DFT (LDA) and tight binding. The bands are filled such that there is one hole per site. (b) Conventional unit cell of the tetragonal phase of RbO_2 . (c) Schematic showing tight binding hopping parameters in meV. Circles represent O_2 anions in a plane perpendicular to the molecular axis, triangles represent O_2 anions in the nearest planes above or below, Rb not shown. (d) Isosurface of the x Wannier function in its local environment. (b) and (d) produced with Vesta [16].

orthorhombic and monoclinic crystal structures that are all slight distortions of the tetragonal phase [15].

The standard LDA calculation for RbO_2 produces a half-metallic (ferromagnetic) state in the averaged unit cell [13], or an antiferromagnetic metal in a Rb_2O_4 supercell, in contrast to experimental reports that MO_2 compounds are insulating [12]. As seen in Fig. 1a, the O_2 bands near the Fermi level have a bandwidth of about 1 eV and are well separated from other bands. These bands contain 3 electrons per O_2 ion, so the occupations of the x and y (hereafter $|x\rangle_x$ and $|y\rangle_y$) orbitals are frustrated and likely related to the structural transitions, as well as the Jahn-Teller distortion that tilts the O_2 ions. Since the relevant bands are so narrow and the system is Mott insulating, one might consider the use of the LDA+U method [1], but since the typical implementation of LDA+U in DFT codes uses interactions between onsite atomic orbitals and the appropriate interactions in MO_2 would be between molecular orbitals, a straightforward application of LDA+U fails to produce the correct ground state [11].

We used the FPLO code [17] to construct a tight-binding Hamiltonian by projecting Wannier functions using symmetry projected orbitals [18, 19] corresponding to the two O_2 molecular orbitals in the primitive cell in a paramagnetic LDA calculation. This al-

lows tight-binding hopping parameters to be calculated directly. We consider only the four most relevant hoppings, two for nearest neighbors ($t_{xx} = \langle \psi | \hat{H} | \psi_{1x} \rangle$ and $t_{xy} = \langle \psi | \hat{H} | \psi_{1y} \rangle$, where $\mathbf{R}_1 = \frac{1}{2}(a\hat{x}; a\hat{y}; c\hat{z})$) and two for second neighbors in the plane ($t_{xx} = \langle \psi | \hat{H} | \psi_{2x} \rangle$ and $t_{yy} = \langle \psi | \hat{H} | \psi_{2y} \rangle$ with $\mathbf{R}_{2x} = a\hat{x}$ and $\mathbf{R}_{2y} = a\hat{y}$). The LDA spin-unpolarized band structure and our tight-binding band structure with four parameters are shown in Fig. 1a. A schematic for the hopping channels used in the tight-binding model is shown in Fig. 1c with the numerical values of the hoppings. Note that the largest hopping is t_{xy} , which represents nearest neighbor hopping from $|x\rangle_i$ to $|y\rangle_j$ orbitals. Second neighbor hoppings from $|x\rangle_i$ to $|y\rangle_j$ are forbidden by symmetry. There are 8 first neighbors with t_{xy} hopping, compared to 2 each for t_x and t_y , and since $8|t_{xy}| > 2|t_x| + 2|t_y|$, this would suggest that the strongest AFM coupling is between nearest neighbor spin ordering. Previous neutron diffraction studies [20] on KO_2 show magnetic ordering consistent with nearest neighbor spin ordering.

The non-interacting Hamiltonian is 2x2, with values

$$H_{xx}^0 = \begin{pmatrix} 8t_{xx}(\mathbf{k}) & 2t \cos k_x & 2t \cos k_y \end{pmatrix} \quad (1)$$

$$H_{yy}^0 = \begin{pmatrix} 8t_{xx}(\mathbf{k}) & 2t \cos k_x & 2t \cos k_y \end{pmatrix} \quad (2)$$

$$H_{xy}^0 = \begin{pmatrix} 4t_{xy} \cos \frac{1}{2}k_z & \sin \frac{1}{2}k_x & \sin \frac{1}{2}k_y \end{pmatrix} \quad (3)$$

where we define the nearest neighbor structure factor

$$(\mathbf{k}) = \cos \frac{1}{2}k_x \cos \frac{1}{2}k_y \cos \frac{1}{2}k_z : \quad (4)$$

The interacting Hamiltonian is

$$H = \sum_{i,j} t_{i,j} c_i^\dagger c_j + \frac{1}{2} U \sum_i n_i n_i \quad (5)$$

where i,j run over sites and $i,j \in \{x,y\}$. We apply second-order perturbation theory to H to get an effective Kugel-Khomskii (KK) [21] type Hamiltonian $H_{KK} = H_{KK}^{nn} + H_{KK}^{nnn}$ for nearest and next nearest neighbor interactions,

$$H_{KK}^{nn} = \sum_{\langle i,j \rangle} \frac{1}{2} (J_{xy} + J_{xx}) S_i \cdot S_j + \frac{3}{4} J_{xy} (S_i^x S_j^x + S_i^y S_j^y) + \frac{1}{4} J_{xx} (S_i^x S_j^x + S_i^y S_j^y) + \frac{1}{2} (J_{xx} - J_{xy}) \sum_i S_i^z S_i^z + \frac{1}{4} \sum_i S_i^z S_i^z \quad (6)$$

$$H_{KK}^{nnn} = \sum_{\langle i,j \rangle} \frac{1}{4} J_s S_i \cdot S_j + \frac{3}{4} J_d \sum_i S_i^z S_i^z + \frac{1}{4} J_d \sum_i S_i^z S_i^z + J_I (S_i^x S_j^x + S_i^y S_j^y) S_i \cdot S_j + \frac{1}{4} J_I \sum_i S_i^z S_i^z \quad (7)$$

in terms of parameters $J_{xy} = 4t_{xy}^2/U$, $J_{xx} = 4t_{xx}^2/U$, $J = 4t^2/U$, $J_s = J + J$ where term with

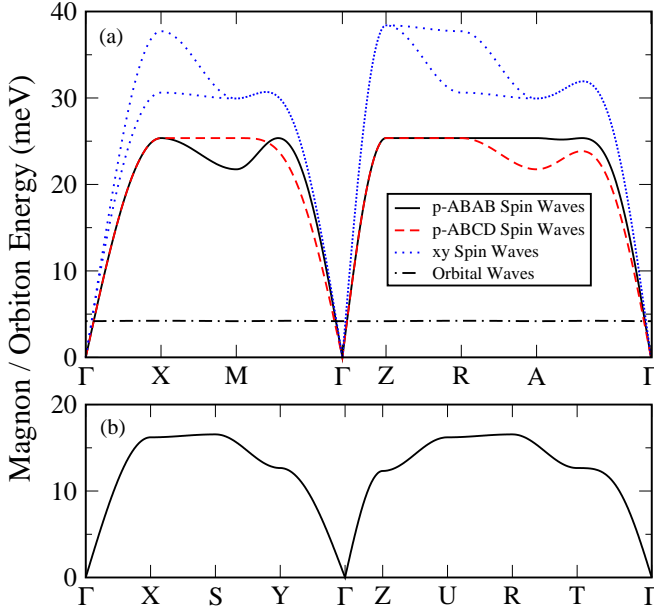


FIG. 2. (Color online) (a) Spin wave spectrum for RbO_2 for p-type ordering for both stackings as described in text (black solid, ABAB stacking and red dashed, ABCD stacking), and spin wave spectrum for xy ordering (blue dotted). Also, the nearly dispersionless orbital spectrum is shown for p-type orderings (black dash-dot line). (b) Spin wave spectrum for ferroorbital ordering, which is orthorhombic symmetry.

a single operators have been neglected. The parameter $J_d = (J - J')$ depends on the direction of the bond between i and j . The operators can be represented as Pauli matrices that operate in orbital space. For numerical results, we select $U = 3$ eV, which is equivalent to $U_e = U - J$ for intraorbital U and Hund's exchange J found previously [13] for the O_2 orbitals in KO_2 via the constrained LDA method [22]. This gives $J_{xx} = 1.54$ meV, $J_{xy} = 4.8$ meV, $J = 3.89$ meV, and $J' = 0.34$ meV.

Unlike previous studies [23–26] on the KKH Hamiltonian, which contained only a single parameter t for both intraorbital and interorbital hopping, we consider here a KKH-type Hamiltonian where the hoppings between orbitals channels are significantly different than hoppings within an channel, as shown in Fig. 1. One previous study [26] concluded that due to unusual symmetries present, the KKH Hamiltonian could not describe the observed order and gapped excitations. In the present work, the broken symmetry of the hoppings in this model should avoid these difficulties. These hoppings will lead to the orbital ground state having a significant impact on the spin wave dispersion, which should be measurable in experiment.

To proceed with spin/orbital wave theory a reference ground state for both the spin and orbital system must be chosen. From here on, we will consider the electronic structure from the hole perspective, so that there is a

single hole per site. We restrict our magnetic order to be antiferromagnetic between with nearest neighbors.

The ground state orbital ordering for this model is where antiferroorbital (AFO) ordering occurs in planes so that a given site with, say, x_i occupied would have second neighbors (first neighbors in the plane) with y_i occupied. We refer to this ordering as p-type. This ordering frustrates the first neighbor orbitals, so alternate stackings of the planes will be very close in energy and may be degenerate. For these orderings, the spin wave dispersion ω_k^p and orbital wave dispersion ω_k^o are given by

$$\omega_k^p = \frac{q}{(8J)^2 [4J_{xy} m(k) + 4J_{xx} n(k)]^2} \quad (8)$$

$$\omega_k^o = \frac{q}{J_s^2 - \frac{1}{2}J_{I2}(k)^2} \quad (9)$$

where $J_I = \frac{P}{J - J'}$ and $J_{I2}(k) = \frac{1}{2}(\cos k_x + \cos k_y)$. where the effect of different stackings is contained in the structure factors $m(k)$ and $n(k)$. First we consider the case of ABAB stacking, where any given site has the same orbital occupation as the sites at displacements $(0;0;c)$ and $(0;0;-c)$ from it. This results in structure factors given by

$$\begin{aligned} m(k)^{ABAB} &= \cos \frac{1}{2}(k_x + k_y) \cos(\frac{1}{2}k_z) \\ n(k)^{ABAB} &= \cos \frac{1}{2}(k_x - k_y) \cos(\frac{1}{2}k_z): \end{aligned} \quad (10)$$

An alternate stacking, ABCD, where each site has the opposite orbital occupation as the sites above and below in the z direction, has structure factors of

$$\begin{aligned} m(k)^{ABCD} &= \cos \frac{k_x}{2} \cos \frac{k_y}{2} \cos \frac{k_z}{2} + \sin \frac{k_x}{2} \sin \frac{k_y}{2} \sin \frac{k_z}{2} \\ n(k)^{ABCD} &= \cos \frac{k_x}{2} \cos \frac{k_y}{2} \cos \frac{k_z}{2} - \sin \frac{k_x}{2} \sin \frac{k_y}{2} \sin \frac{k_z}{2}: \end{aligned} \quad (11)$$

The dispersions are depicted in Fig. 2a.

An alternate orbital ordering we consider is where the ordering within planes are ferroorbital (FO) ordering. This ordering is not stable to orbital fluctuations within our KKH model, however it may be stabilized in RbO_2 by effects not considered here, such as the Jahn-Teller distortion that causes the canting of the O_2 molecules. This ordering is of particular interest because if the stacking of planes is AFO, then the nearest neighbor spin exchange is maximized. With this orbital ordering (hereafter referred to as xy ordering), the spin sublattices have different dispersions due to the swapping of J and J' in each plane. The Kugel-Khomskii Hamiltonian yields a spin wave dispersion of

$$\omega_k^{xy} = \frac{q}{A_m^2 (8J_{xy}(k))^2 - A_d} \quad (12)$$

with $A_m = 8J_{xy} [J_s - \frac{1}{2}(\cos k_x + \cos k_y)]$ and $A_d = (J - J') [\cos k_x - \cos k_y]$, and is shown in Fig. 2a.

Thus far, the orderings considered all preserve tetragonal symmetry, but orthorhombic and monoclinic low temperature phases of RbO_2 exist. The natural orbital ordering we consider is FO ordering for every site in the crystal, hereafter called xx ordering, which is orthorhombic symmetry. This has spin-wave dispersion $\epsilon_k^{\text{xx}} = \frac{A_k^2}{4} - \frac{B_k^2}{4}$ where $A_k = 8J_{\text{xx}} + \frac{1}{2}(J_s - J \cos k_x - J \cos k_y)$ and $B_k = 8J_{\text{xx}}(k)$. Again, this conformation is not stable with respect to orbital fluctuations, but it may be stabilized by effects not considered here, which a study of KO_2 indicates is the case [27]. The magnon dispersions is shown in Fig. 2b.

	Orbital Order			
	xx	xy	p-ABAB	p-ABCD
E_0	-12.680	-12.680	-14.795	-14.795
E_s	-0.411	-3.266	-2.333	-2.288
E_o	0	0	-0.010	-0.010
E_{tot}	-13.091	-15.946	-17.138	-17.093

TABLE I. Energies contributing to the ground state energy in meV. E_0 is the classical ground state energy, E_s (E_o) is the quantum correction from spin (orbital)-wave theory.

The ground state energies for these four orbital orderings are listed in table I, where we find that the ABAB stacking of planar orbital ordering is the lowest energy. For an average nearest neighbor spin exchange of $J = 3.17$ meV (in p-type orderings), high temperature series expansion [28] would predict $T_N = 1.4J = 51\text{K}$, much higher than the observed $T_N = 15\text{K}$. The frustrated exchanges within planes would reduce this value somewhat, but not enough to give a prediction reasonably close to the experimental transition.

As expected, the two stackings examined for the planar orbital ordering are very nearly degenerate, with only quantum fluctuations in the spin waves breaking the degeneracy at this level of approximation. It is rather clear that due to the strong asymmetry between hopping within an orbital channel and hopping between orbital channels, the orbital ground state significantly impacts the spin wave spectrum and could be inferred from a measurement of the low temperature magnons. The planar orbital orderings don't significantly impact the spin wave dispersion, so even if the stacking is disordered magnon excitations should be coherent. Energetically the next state above p-type ordering is the xy ordering, which is 1.2 meV (14 K) higher in energy than p-type ordering. Above this temperature orbital domains should proliferate. The strong modulation of exchange constants at the domain boundaries should nucleate magnetic domains [29], leading to the low observed Neel temperature of RbO_2 of 15 K.

Orbitons are quite difficult to measure experimentally. They do not couple directly to neutrons, the standard

measurement technique for magnons. Recently orbitons have been measured in titanates via X-rays [30], but the inference of the orbital dispersion is very indirect. The measured dispersion is negligible, suggesting [30] that X-rays modulate bonds resulting in a much bigger scattering from two-orbitons than from single orbitons. It may be that in narrow band molecular oxide systems the X-rays will create single orbiton excitations with all bond modulation inside a unit cell. If that is the case, the X-ray measured dispersion in RbO_2 should be clearly observable, if a similar experiment can be done. Neglected here is the Jahn-Teller effect which rotates the O_2 molecules and breaks the orbital degeneracy, which will select a particular ground state orbital ordering.

We have examined independent magnon and orbiton excitations in RbO_2 within spin/orbital wave theory, finding considerable coupling between the easily measured magnon excitations and the difficult to measure orbital ground state. This strong coupling arises from the large anisotropy in the hopping parameters in the O_2 bands. This indicates that MO_2 materials are attractive for studying the interplay between orbital ordering and p-electron magnetism. E.R.Y. and W.E.P. were supported by DOE SciDAC Grant No. DE-FC02-06ER25794. The authors would like to thank J. Kunes, R.T. Scalettar, and C. Felser for stimulating conversation.

-
- [1] V. I. Anisimov, F. Aryasetiawan, and A. I. Lichtenstein, J. Phys.: Condens. Matter 9, 767 (1997).
 - [2] A. Georges, G. Kotliar, W. Krauth, and M. J. Rozenberg, Rev. Mod. Phys. 68, 13 (1996).
 - [3] J. E. Medvedeva, M. A. Korotin, V. I. Anisimov, and A. J. Freeman, Phys. Rev. B 65, 172413 (2002).
 - [4] I. S. Elmov, S. Yunoki, and G. A. Sawatzky, Phys. Rev. Lett. 89, 216403 (2002).
 - [5] V. Pardo and W. E. Pickett, Phys. Rev. B 78, 134427 (2008).
 - [6] R. Pentcheva and W. E. Pickett, Phys. Rev. B 74, 035113 (2006).
 - [7] H. Peng, H. J. Xiang, S. H. Wei, S. S. Li, J. B. Xia, and J. Li, Phys. Rev. Lett. 102, 017201 (2009).
 - [8] O. Volnianska and P. Boguslawski, Phys. Rev. B 77, 220403(R) (2008).
 - [9] J. J. Attema, G. A. de Wijs, G. R. Blake, and R. A. de Groot, J. A. Chem. Soc. 127, 16325 (2005).
 - [10] J. J. Attema, G. A. de Wijs, and R. A. de Groot, J. Phys.: Condens. Matter 19, 165203 (2007).
 - [11] J. W. Interlik, G. H. Fecher, C. A. Jenkins, C. Felser, K. D. C. Mühle, M. Jansen, L. M. Sandratskii, and J. Kubler, Phys. Rev. Lett. 102, 016401 (2009).
 - [12] M. Jansen, R. Hagenmayer, and N. Korber, C. R. Acad. Sci. Paris 2, 591 (1999).
 - [13] I. V. Solovyev, New J. Phys. 10, 013035 (2008).
 - [14] M. Labhart, D. Raoux, W. Kanizig, and M. A. Bosch, Phys. Rev. B 20, 53 (1979).
 - [15] M. Rosenfeld, M. Ziegler, and W. Kanizig, Helv. Phys.

- Acta 51, 299 (1978).
- [16] K. Mönma and F. Izumi, *J. Appl. Crystallogr.* 41, 653 (2008).
- [17] K. Koepf and H. Eschrig, *Phys. Rev. B* 59, 1743 (1999).
- [18] W. Ku, H. Rosner, W. E. Pickett, and R. T. Scalettar, *Phys. Rev. Lett.* 89, 167204 (2002).
- [19] E. R. Ylvisaker and W. E. Pickett, *Phys. Rev. B* 74, 075104 (2006).
- [20] H. G. Smith, R. M. Nicklow, L. J. Raubenheimer, and M. K. Wilkinson, *J. Appl. Phys.* 37, 1047 (1966).
- [21] K. I. Kugel and D. I. Khomskii, *Sov. Phys. Usp.* 25, 231 (1982).
- [22] O. Gunnarsson, O. K. Andersen, O. Jepsen, and J. Zaanen, *Phys. Rev. B* 39, 1708 (1989).
- [23] G. Khaliullin and V. Oudovenko, *Phys. Rev. B* 56, R14243 (1997).
- [24] L. F. Feiner, A. M. Oles, and J. Zaanen, *Phys. Rev. Lett.* 78, 2799 (1997).
- [25] A. B. Harris, A. Aharony, O. Entin-Wohlman, I. Y. Korenblit, and T. Yildirim, *Phys. Rev. B* 69, 094409 (2004).
- [26] A. B. Harris, T. Yildirim, A. Aharony, O. Entin-Wohlman, and I. Y. Korenblit, *Phys. Rev. B* 69, 035107 (2004).
- [27] M. Kim, B. H. Kim, H. C. Choi, and B. I. Min, *arXiv:0911.5677* (2009).
- [28] J. Oitmaa and W. Zheng, *Phys. Rev. B* 69, 064416 (2004).
- [29] I. I. Mazin and M. D. Johannes, *Nat. Phys.* 5, 141 (2009).
- [30] C. Ulrich, L. J. P. Ament, G. Ghiringhelli, L. Braicovich, M. M. Sala, N. Pezzotta, T. Schmitt, G. Khaliullin, J. van den Brink, H. Roth, et al, *Phys. Rev. Lett.* 103, 107205 (2009).